

**PERFORMANCE OF ZINC OXIDE-
POLYANILINE HETEROJUNCTION FOR UV
PHOTODETECTION**

by

RAWNAQ ADNAN TALIB

**Thesis submitted in fulfillment of the requirements
for the degree of
Doctor of Philosophy**

December 2016

ACKNOWLEDGEMENT

First and foremost, I would like to thank Allah for granting me health and patience to complete this doctor project. I would like to express my gratitude for the guidance and support from my main supervisor, Professor. Dr. Mat Johar Abdullah, during this study. He is an extremely helpful and encouraging advisor, who helped me through difficult times in my research work. Thanks again prof. for having your door open every time I needed help, even when you never had the time, you always made it. I would also like to express my appreciation to my co-supervisor Dr. Naser M. Ahmed for his guidance and support throughout my study. I would like to express my deepest thanks to my friends Husam Shakir and Sabah M. Mohammad for their excellent cooperation to achieve our research, many thanks for their help and support. I offer my appreciation to School of Physics Universiti Sains Malaysia especially Solid State lab and (NOR) lab staff: Mahfuzah Binti Mohamad Fuad, Ee Bee Choo, Mohd Anas, Yus Hamdan, Abdul Jamil, Noor Aswafi and Sayed Mohamad, for their technical assistance and I am totally indebted for their wonderful help. I would like to thank University of Basra for the study leave to complete this Ph.D. degree and the lecturers and staff in Polymer Research Center. Far in distance and connected in hearts, I wish to express my deepest thanks to my dear father, mother, sisters and all my relatives for their kindness, long time moral support, and unconditional love. Last but not the least, I would like to thank all my friends and colleagues who supported me and helped me at the School of Physics in Universiti Sains Malaysia and University of Basra.

TABLE OF CONTENTS

ACKNOWLEDGEMENT	ii
TABLE OF CONTENTS	iii
LIST OF TABLES	viii
LIST OF FIGURES	x
LIST OF ABBREVIATIONS	xvi
LIST OF SYMBOLS	xx
ABSTRAK	xxii
ABSTRACT	xxiv
CHAPTER 1: INTRODUCTION	1
1.1 Introduction.....	1
1.2 Motivations and Problem statement	4
1.3 Objective of this research	6
1.4 Originality of the research	7
1.5 Scope of study.....	8
1.6 Thesis outline	8
CHAPTER 2: BACKGROUND AND LITERATURE REVIEW	9
2.1 Introduction.....	9
2.2 Background of polymers.....	9
2.3 Background of conducting polymers.....	10
2.3.1 Conduction mechanism of conducting polymers	13

2.3.2	Polyaniline (PAni)	14
2.4	Zinc Oxide (ZnO)	18
2.4.1	Growth mechanism of ZnO(NRs) by Chemical bath deposition (CBD).	21
2.4.2	Twining ZnO structures	23
2.4.3	Growth mechanism of twin ZnO	25
2.5	Composite materials and ZnO-PAni Composite	26
2.6	p-n Junction of n-ZnO and p-PAni	31
2.7	Photodetectors	36
2.7.1	Photoconductor mechanism	37
2.7.2	n (ZnO) - p (PAni) photodiode	38
2.7.3	Important parameters of photodetectors	39
2.7.4	Photodetector based on ZnO-PAni	40
CHAPRER 3: METHODOLOGY AND INSTRUMENTATION		42
3.1	Introduction	42
3.2	Preparation of the twin ZnO-PAni composites	43
3.2.1	Experimental	44
3.3	Cleaning of substrates	45
3.3.1	Preparation and Cleaning of Glass and PET substrates	45
3.3.2	Silicon wafer cleaning	45
3.4	Photoelectrochemical etching (PECE) cell	46
3.5	ZnO-PAni Composite Film	47
3.5.1	Spin coating	47
3.5.2	Casting	48
3.6	Synthesis of ZnO (NRs) on Various Substrates	49

3.6.1	Deposition of ZnO seed layer by RF-sputtering	49
3.6.2	Annealing process of the ZnO seed layer	51
3.6.3	Synthesis of ZnO (NRs) using CBD	52
3.7	Fabrication of n-ZnO/p-PAni heterojunction.....	53
3.7.1	Oxidation of Si wafer	53
3.7.2	Growth n-ZnO (NRs)/ p-PAni on different substrates	54
3.8	Fabrication of UV photodetector.....	56
3.9	Instrumentations	59
3.9.1	X-ray diffraction (XRD)	60
3.9.2	Field emission scanning electron microscopy (FESEM)	62
3.9.3	Fourier transform infrared spectroscopy (FTIR).....	64
3.9.4	Optical absorption	65
3.9.5	Photoluminescence	67
3.9.6	Raman spectroscopy.....	68
3.9.7	Hall effect.....	69
3.9.8	Measurements of UV photodetector.....	69
CHAPTER 4: RESULTS AND DISCUSSIONS		
ZnO-and ZnO-PAni Composites.....		
		71
4.1	Introduction.....	71
4.2	Characterization of twin ZnO-PAni composites.....	71
4.2.1	X-ray diffraction analysis	71
4.2.2	FESEM observation.....	75
4.2.3	FTIR spectroscopy analysis	80
4.2.4	Raman spectroscopy analysis.....	83
4.3	Twin ZnO and ZnO-PAni composites of UV photodetection properties.	86

4.3.1	Surface morphology of porous Silicon using FESEM	86
4.3.2	UV photodetector measurements	88
4.4	FESEM of microparticle ZnO-PAni composites	94
4.5	UV-Vis spectroscopy of ZnO-PAni (microparticle) composites	98
4.6	UV photodetection of ZnO-PAni (microparticles) composites	101
4.7	Summary	115

CHAPTER 5: RESULTS AND DISCUSSION

ZnO Nanorods (NRs) and ZnO (NRs)/Polyaniline Heterojunctions 118

5.1	Introduction.....	118
5.2	Effect of growth time on the structure, optical and photo-response properties of ZnO NRs deposited on various substrates.	118
5.2.1	X-ray diffraction analysis	118
5.2.2	Morphological observations.....	122
5.2.3	Optical properties	123
	5.2.3(a) Photoluminescence (PL) characterization of ZnO (NRs) growth on different substrates.....	123
	5.2.3(b) Raman spectroscopy	126
5.2.4	UV photodetector sensitivity measurements	128
5.3	ZnO Nanorods/Polyaniline heterojunctions.....	137
5.3.1	FESEM characterization of n-ZnO (NRs)/ p-PAni	137
5.3.2	XRD characterization of n-ZnO (NRs)/ p-PAni on different substrates.....	140
5.3.3	Optical properties.	142
	5.3.3(a) Photoluminescence (PL) characterization of ZnO(NRs)/PAni on different substrates.....	142
5.3.4	Hall effect of Polyaniline (PAni).	144
5.3.5	UV photodetector sensitivity measurements of n-ZnO/p-PAni junction	145

5.4 Summary 152

CHAPTER 6: CONCLUSION AND FUTURE WORKS 153

6.1 Conclusions 153

6.2 Future works 156

REFERENCES 158

LIST OF PUBLICATIONS

LIST OF TABLES

	Page
Table 4.1: Structural properties of ZnO and ZnO-PAni composites	75
Table 4.2: Characteristics frequencies of PAni and ZnO-PAni composites.	82
Table 4.3: Raman wave numbers (cm^{-1}) of ZnO and ZnO-PAni composites.	85
Table 4.4: The response and fall times, sensitivity, responsivity, and gain of UV photodetector under different bias voltages of the PS, PAni/PS, twin ZnO and ZnO-PAni composites on PS substrate.	94
Table 4.5: Summary of energy gap of PAni and ZnO-PAni composites from optical absorption spectra.	101
Table 4.6: The response time, fall time, sensitivity, and gain of the Pt-(ZnO-PAni) composites-Pt, Pt-PAni-Pt, and Pt-Si-Pt at various bias voltages.	112
Table 4.7: The response time, fall time, sensitivity, and gain of the RF sputtered ZnO film based photodetector at various bias voltages.	115
Table 5.1: Structural characteristics of ZnO NRs grown onto different substrates.	122
Table 5.2: Summarized data from PL spectra of ZnO (NRs).	125
Table 5.3: The turn-on voltage of UV photodetector based on ZnO (NRs) at (2h and 3h) under different substrates.	132
Table 5.4: The response and fall times, sensitivity, and gain of UV photodetector based on ZnO (NRs) (2h and 3h) under different bias voltages grown on different substrates.	136
Table 5.5: Lattice constant, strain and crystallite size of the ZnO (NRs) grown on the ZnO seed/ PAni along the c-axis.	142
Table 5.6: Turn-on voltage of n-ZnO/p-PAni junction under light grown onto different substrates.	149
Table 5.7: n-ZnO/p-PAni junction parameters of dark and under light of ZnO NRs/ZnO seed/PAni grown onto different substrates.	150
Table 5.8: The response time, fall time, sensitivity, and gain of n-ZnO/p-PAni.	151

Table 5.9: Photodiode properties for the fabricated n-ZnO/p-PAni junction
in comparison with other reported.151

LIST OF FIGURES

	Page
Figure 1.1: The schematic structure of photoconductor [19].	3
Figure 1.2: The schematic of MSM photodiode structure [19].	4
Figure 1.3: The schematic of p-n junction photodiode [19].	4
Figure 2.1: Structure of conducting polymers [50].	12
Figure 2.2: Application of conducting polymers.	12
Figure 2.3: Band structure in an electronically conducting polymer.	14
Figure 2.4: Formation of a polaron and a bipolaron for polyacetylene.	14
Figure 2.5: The general structure of polyaniline.	15
Figure 2.6: Chemical polymerization of PANi.	17
Figure 2.7: Electrochemical polymerization [78].	18
Figure 2.8: Crystal structure of ZnO (a) zinc blend, and (b) hexagonal wurtzite structure [90, 91].	19
Figure 2.9: Different type of defects in crystalline material.	20
Figure 2.10: Schematic illustration of the ZnO(NRs) growth by CBD.	22
Figure 2.11: ZnO twin structure[99].	23
Figure 2.12: Schematic of growth process of the ZnO twin-rods [104].	26
Figure 2.13: A UV- detection mechanism of ZnO (NRs). (a) Darkness and (b) UV illumination [129].	38
Figure 2.14: Calculation of rise time and full time of a pulse current.	40
Figure 3.1: Flowchart of the fabrication and characterization of UV photodetector based on ZnO-PAni composites.	43
Figure 3.2: Preparation of ZnO-PAni composite.	44
Figure 3.3: Diamond scribe used for cutting Silicon wafer substrate to small pieces.	46

Figure 3.4:	Schematic illustration of the photoelectrochemical (PECE) cell used for fabricating PS substrate.	47
Figure 3.5:	Spin Coater used to deposit uniform (ZnO-PAni) composites thin films on flat substrates.	48
Figure 3.6:	Vibration machine used to deposit uniform (ZnO-PAni) composites thin films on flat substrates without spin.	49
Figure 3.7:	Photograph of the RF-sputtering system to deposit ZnO (seed layer) for growing ZnO (NRs) and used for depositing electrode (Pt) for fabricating MSM UV detector.	50
Figure 3.8:	Schematic of RF- sputtering [137].	51
Figure 3.9:	Photograph of the thermal annealing furnace system used for annealing ZnO seed layer.	52
Figure 3.10:	Schematic illustration for design of growth ZnO(NRs) by CBD.	53
Figure 3.11:	Photograph of oxidation furnace system used for oxidizing Si substrate.	54
Figure 3.12:	Schematic illustration for design of preparation ZnO/PAni hetrojunction.	56
Figure 3.13:	Schematic illustration of the UV photodetector based on twin ZnO-PAni composite on PS/Si substrate.	57
Figure 3.14:	Schematic illustration of the UV photodetector based on micro particle ZnO-PAni composite on various substrates.	57
Figure 3.15:	Schematic illustration of the UV photodetector based on ZnO(NRs) on various substrates.	58
Figure 3.16:	Schematic illustration of the UV photodetector based on n-ZnO(NRs)/p-PAni on various substrates.	58
Figure 3.17:	Schematic diagram of the metal mask used for the fabrication of the metal electrode of MSM photodetector.	59
Figure 3.18:	Photograph of (ZnO-PAni) composites on silicon substrate as UV detection.	59
Figure 3.19:	Schematic of X-ray diffraction [139].	61
Figure 3.20:	Schematic diagram of a scanning electron microscopy [140].	63
Figure 3.21:	Schematic optical of a FTIR system.	65

Figure 3.22:	Schematic illustration of UV-Vis spectrophotometer.	66
Figure 3.23:	PL instrument setup configuration [143].	67
Figure 3.24:	Schematic diagrams of the two types of scattering processes, the E_0 and $E_0+h\nu$ are initial and final states, respectively.	68
Figure 3.25:	Schematic diagram of the Hall effect system.	69
Figure 3.26:	Schematic of experimental setup of photodetector measurement.	70
Figure 4.1:	XRD patterns of pure ZnO and ZnO-PAni composites at different ratio of PAni.	74
Figure 4.2:	FESEM images and EDX data of pure ZnO and ZnO-PAni composites: (a) ZnO, (b) ZnO-5% PAni, (c) ZnO-10% PAni, (d) ZnO-15% PAni, and (e) ZnO-20% PAni.	76
Figure 4.3:	Flowchart of growth twin ZnO rods.	79
Figure 4.4:	FTIR spectra of pure PAni, ZnO-5% PAni, and ZnO-15% PAni composites.	81
Figure 4.5:	Raman spectrum of ZnO and Composites.	84
Figure 4.6:	A schematic showing possible linkages between surface defect of ZnO and PAni [28].	85
Figure 4.7:	FESEM images of porous silicon with etching times from 5 min to 60 min.	87
Figure 4.8:	Cross sectional micrographs of (a) PS without twin, (b) PS with twin at magnification 20k, and (c) at magnification 50k.	88
Figure 4.9:	Spectral response shows the responsivity curve of the fabricated MSM ZnO/PS PD as a function of incident light wavelength, at a fixed applied bias of 5 V.	89
Figure 4.10:	(a) Current-Voltage characteristics of the PS, PAni/PS, twin ZnO, and twin ZnO-PAni composites under dark and UV illumination, (b) the switching property (ON/OFF) of the PS, PAni/PS, twin ZnO and twin ZnO-PAni composites under pulsed UV light at various bias voltages.	92
Figure 4.11:	FESEM images of microparticle ZnO-PAni composites deposited on different substrates: glass, PET, and Si.	95
Figure 4.12:	Morphology of the ZnO-PAni composites surface of the hexagonal particles.	98

Figure 4.13:	UV-Vis absorption spectra of PANi and ZnO-PANi composites.	100
Figure 4.14:	$(\alpha h\nu)^2$ as a function of photon energy ($h\nu$) for PANi and ZnO-PANi composites.	100
Figure 4.15:	Responsivity of the fabricated MSM ZnO-PANi composite PD as a function of incident light wavelength, at a fixed applied bias of 5 V.....	102
Figure 4.16:	Current-Voltage (I-V) characteristic in dark and under UV illumination (400 nm) of Pt-(ZnO-PANi) composites-Pt on glass substrate.	103
Figure 4.17:	Current-Voltage (I-V) characteristic in dark and under UV illumination (400 nm) of Pt-(ZnO-PANi) composites-Pt on PET substrate.	104
Figure 4.18:	Current-Voltage (I-V) characteristic in dark and under UV illumination (400 nm) of Pt-(ZnO-PANi) composites-Pt on Si substrate.	105
Figure 4.19:	The repeatability characteristic (ON/OFF) of Pt-(ZnO-PANi) composites-Pt on glass substrate under pulsed UV light (400 nm) at various bias voltages.	106
Figure 4.20:	The repeatability characteristic (ON/OFF) of Pt-(ZnO-PANi) composites-Pt on PET substrate under pulsed UV light (400 nm) at various bias voltages.	107
Figure 4.21:	The repeatability characteristic (ON/OFF) of Pt-(ZnO-PANi) composites-Pt on Si substrate under pulsed UV light (400 nm) at various bias voltages.	108
Figure 4.22:	The I-V and repeatability(ON/OFF) characteristic of PANi film on glass, PET, and Si substrate under pulsed UV light at various bias voltages.....	109
Figure 4.23:	Schematic representation of energy levels and processes involved under UV illumination.	109
Figure 4.24:	The (I-V) and Repeatability characteristic (ON/OFF) of Si substrate under pulsed UV light at various bias voltages.....	110
Figure 4.25:	The repeatability characteristic (ON/OFF) of RF-sputtered ZnO film on (a) glass, (b) PET, and (c) Si substrate under pulsed UV light at various bias voltages.	111
Figure 5.1:	XRD patterns of ZnO (NRs) on various substrates at (a) 2h growth time.	120

Figure 5.2:	FESEM images of ZnO (NRs) deposited onto various substrates: (a) 2h growth time the diameter and length of rods are approximal 50nm and 600 nm, (b) 3h growth time the diameter and length of rods are approximal 70nm and 900 nm.	123
Figure 5.3:	The PL spectra of the ZnO (NRs) on various substrates at: (a) 2h growth time.	125
Figure 5.4:	Raman spectra of ZnO (NRs) grown on various substrates at: (a) 2h growth time.	127
Figure 5.5:	Responsivity spectra of the ZnO (NRs) on (a) PET and (b) Si substrate as MSM photodetectors.	129
Figure 5.6:	I-V characteristics of Pt-ZnO (NRs)-Pt devices fabricated from ZnO (NRs) deposited onto various substrates: (a) 2h growth time.	131
Figure 5.7:	UV ON/OFF photo-response of ZnO (NRs) arrays grown onto various substrates at: (a) 2h growth time.	134
Figure 5.8:	The repeatability characteristic (ON/OFF) of UV photodetector based on ZnO (NRs) arrays (3h) on Si substrate upon exposure to UV light at zero bias voltage.	136
Figure 5.9:	Cross-section of ZnO (NRs)/PAni on SiO ₂ /Si substrate.	138
Figure 5.10:	Images of ZnO nanorods/PAni films formed at 90oC for different growth duration; (a) 1h, (b) 2h, and (c) 3h.	139
Figure 5.11:	FESEM images of ZnO nanorods/PAni grown at; (a) 50 °C and (b) 70 °C (the growth time was 3h).	140
Figure 5.12:	X-ray diffraction (XRD) spectra for the ZnO (NRs)/PAni films on (a) glass, (b) PET, and (c) SiO ₂ /Si substrate.	141
Figure 5.13:	Photoluminescence spectrum of ZnO (NRs)/ZnO seed/PAni on (a) glass, (b) PET, and (c) SiO ₂ /Si substrate.	143
Figure 5.14:	(a) Hall effect of PAni (Accent HL5500PC).	144
Figure 5.15:	Spectral response shows the responsivity curve of the fabricated n-ZnO/p-PAni PD as a function of incident light wavelength, at a fixed applied bias of 5 V.	147
Figure 5.16:	I-V characteristics under dark and UV illumination of n- ZnO (NRs)/ ZnO seed/ p-PAni on (a) glass, (b) PET, and (c) SiO ₂ /Si substrate.	148

Figure 5.17:	Semi-logarithmic plot of the current as a function of the bias voltage (I-V) of the n- ZnO (NRs)/ZnO seed/ p-PAni on (a) glass, (b) PET, and (c) SiO ₂ /Si substrate in dark and UV illumination.	149
Figure 5.18:	Photoresponse of the n-ZnO(NRs)/ ZnO seed/ p-PAni photodetectors under dark and illumination (380 nm) conditions at different bias voltages on (a) glass, (b) PET, and (c) SiO ₂ /Si substrate.	150

LIST OF ABBREVIATIONS

Al	Aluminium
Al ₂ O ₃	Aluminium oxide
NH ₃	Ammonium
NH ₄ OH	Ammonium hydroxide
(NH ₄) ₂ S ₂ O ₈	Ammonium per sulfate
APS	Ammonium persulfate
Ar	Argon
AsF ₅	Arsenic fluoride
Br ₂	Bromine
CdSe	Cadmium Selenide
CdS	Cadmium Sulfide
CaCO ₃	Calcium carbonate
CSA	Camphor sulfonic acid
C	Carbon
CBD	Chemical bath deposition
CVD	Chemical vapor deposition
CB	Conduction band
Cu	Copper
DI	Deionized water
DEA	Diethanolamine
DMF	Dimethylformamide
SDBS	Dodecylbenzensulfonate
N719	Dye-sensitized
ESMs	Egg shell membranes
EDX	Energy dispersive X-ray
C ₂ H ₅ OH	Ethanol
NH ₂ (CH ₂)NH ₂	Ethylenediamine

FeCl ₃	Ferric chloride
FESEM	Field emission scanning electron microscopy
FTO	Fluorine doped tin oxide
FTIR	Fourier transform infrared
FWHM	Full width at half maximum
Ga	Gallium
Au	Gold
He-Cd	Helium- Cadmium
He-Ne	Helium-neon laser
C ₆ H ₁₂ N ₄	Hexamethylenetetramine
HMTA	Hexamethylenetetramine
HUMO	Highest occupied molecular orbital
HCL	Hydrochloride acid
HF	Hydrofluoric acid
PH	Hydrogen ions
H ₂ O ₂	Hydrogen peroxide
OH	Hydroxyl group
In	Indium
ITO	Indium tin oxide
I	Iodine
Fe	Iron
JCPDS	Joint Committee on Powder Diffraction
LEDs	Light Emitting Diodes

LPG	Liquefied petroleum gas
LiOH	Lithium hydroxide
LUMO	Lowest unoccupied molecular orbital
MSM	Metal- Semiconductor-Metal
NPs	Nanoparticles
NRs	Nanorods
NWs	Nanowires
Ni	Nickel
N ₂	Nitrogen
N ₂	Nitrogen
NMP	N-methyl-2-pyrrolidone
O ₂	Oxygen
PATP	P-aminothiophenol
PECE	Photoelectrochemical etching
PL	Photoluminescence
Pt	Platinum
PAni	Polyaniline
PEG	Polyethylene glycol
PET	Polyethylene terephthalate
(C ₂ H ₅ N) _n	Polyethylenimine
PMMA	Polymethylmethacrylate
PEO	Polyethylene oxide
PVA	Polyvinyl alcohol
PVP	Polyvinyl pyrrolidone
PS	Porous silicon
KBr	Potassium bromide

KPS	Potassium peroxydisulfate
PLD	Pulsed laser deposition
RCA	Radio Corporation of America
RF	Radio frequency
RT	Room temperature
SCE	Saturated calomel electrode
Si	Silicon
SiO ₂	Silicon dioxide
Ag	Silver
AgCl	Silver chloride
NaOH	Sodium hydroxide
H ₂ SO ₄	Sulfuric acid
NH ₂ CSNH ₂	Thiourea
TiO ₂	Titanium dioxide
UV	Ultraviolet
UV-Vis	Ultraviolet-visible
VB	Valence band
VPT	Vapor-phase transport
H ₂ O	Water
XRD	X-ray diffraction
Zn	Zinc
Zn(CH ₃ COO) ₂ ·2H ₂ O	Zinc acetate dehydrate
Zn(OH) ₂	Zinc hydroxide
Zn(NO ₃) ₂	Zinc nitrate
Zn(NO ₃) ₂ ·6H ₂ O	Zinc nitrate hexahydrate
ZnO	Zinc Oxide

LIST OF SYMBOLS

T	Absolute temperature
A	Absorbance
α	Absorption coefficient
Å	Angstroms
a.u	Arbitrary unit
D	Average crystallite size
Φ_{β}	Barrier height
K	Boltzmann's constant
°C	Celsius temperature
e^{-}	Charge of electron
h^{+}	Charge of hole
A_0	Constant
I	Current
I-t	Current-Time
I-V	Current-Voltage
I_d	Dark current
θ	Diffraction angle
DC	Direct current
eV	Electron volt
q	Elementary Charge
E_g	Energy gap
β	Full width at half maximum
G	Gain
n	Ideality factor
$I_{UV}/I_{\text{visible}}$	Intensity ratio
d	Inter planar spacing

a, b, c	Lattice constant
c_0	Lattice constant in Z-axis for bulk material
L	Length
B	Magnetic field
ϕ_m	Metal work function
h, k, l	Miller indices
M_w	Molecular weight
V_{O^+}	Monovalent vacancies
O_i	Oxygen interstitial
V_o	Oxygen vacancies
I_{ph}	Photo current
h ν	Photon energy
R	Responsivity
rpm	Revolution per minute
I_s	Saturation current
ϕ_s	Semiconductor work function
S	Sensitivity
ϵ_c	strain
P	The power of the light
δ	Thickness
V	Voltage
W	Watt
λ	Wavelength
w	Weight
Zn_i	Zinc interstitials
V_{zn}	Zinc vacancies

PRESTASI SIMPANG-HETERO ZINK OKSIDA-POLIANILINA UNTUK PENGESANAN FOTO UV

ABSTRAK

Tujuan kajian ini adalah untuk menfabrikasi dan mencirikan komposit dan persimpangan hetero zink oksida-polianilin untuk aplikasi foto-pengesan ultra ungu. Pada mulanya, foto-pengesan berdasarkan komposit ZnO-PAni difabrikasi pada konsentrasi berlainan PAni dari 5 wt % ke 20 wt % menggunakan dua kaedah yang berlainan- kaedah pertama, foto-pengesan berdasarkan komposit kembar (ZnO-PAni) yang dimendapkan ke atas substrat silikon poros (PS). Dalam kaedah kedua, foto-pengesan sinar ungu berdasarkan mikro-partikel komposit ZnO-PAni dihasilkan ke atas substrat kaca, PET, dan silikon (Si) telah difabrikasi. Kaedah pemendapan kimia (CBD) telah digunakan untuk mencerakinkan ZnO (NRs) ke atas substrat kaca, PET dan Si. Kesemua struktur alat ini dicirikan untuk foto-pengesan UV (ultra ungu) menggunakan elektrod platinum (Pt). Keputusan menunjukkan bahawa penambahan PAni dalam komposit berkenaan tidak mengubah struktur heksagonal fasa ZnO, tetapi saiz batang kristal ZnO bertambah lebar dengan peningkatan konsentrasi PAni. Sensitiviti foto-pengesan UV mikro-partikel ZnO dengan 10 wt% PAni ke atas substrat Si adalah 1.5 kali lebih hebat dari tatasusunan ZnO (NRs) yang dicerakin di atas substrat Si, 11.5 kali lebih hebat dari kembar ZnO dengan 15 wt% komposit PAni di atas substrat PS, dan 29.5 kali lebih hebat dari persimpangan p-n yang difabrikasi dengan cara cerakinan di atas substrat n-ZnO (NRs) ke atas p-polianilina (PAni) dan ke atas substrat SiO₂/Si. Prestasi kesemua foto-pengesan yang difabrikasi dikaitkan dengan struktur, morfologi permukaan, substrat dan ciri-ciri optik bahan yang digunakan dan proses foto-pengesan telah dibincangkan. Foto-sensitiviti komposit

ZnO-PAni boleh dipertingkatkan lagi dengan lebih baik daripada alat ZnO apabila diradiasi dengan cahaya ultra ungu, dan satu sebabnya ialah komposit ZnO-PAni memaparkan serapan yang lebih kuat di kawasan ultra ungu kerana kedua-dua ZnO dan PAni boleh diserap oleh cahaya ultra ungu, dan satu sebab lain yang juga penting ialah PAni dalam komposit ZnO-PAni boleh menyumbang kepada pengeluaran lebih banyak penggegaran elektron bebas dalam ZnO, disebabkan oleh kewujudan simpang p-n dalam komposit ZnO-PAni. Foto-sensitiviti komposit ZnO-PAni yang tinggi ke atas substrat Si mungkin disebabkan oleh penyerapan photon di dalam lapisan komposit ZnO-PAni, sementara beberapa elektron mungkin berselerak di persimpangan ZnO-PAni/Si dan seterusnya dibawa ke bahagian Si. Namun demikian, fabrikasi berjaya simpang-hetero ZnO nanorod/polianilina yang berkualiti tinggi, simpang-hetero ZnO nanorod/polianilina yang disejajarkan dan mikropartikel komposit ZnO-PAni ke atas substrat PET yang fleksibel dengan cara mengkaji kebolehaplikasian sebagai pengesan cahaya yang fleksibel, yang memainkan peranan yang sangat penting dalam aplikasi optoelektronik disebabkan oleh ciri-ciri dielektrik yang istimewa, rintangan terhadap hakisan, serta suhu pemprosesan tinggi di antara 196 dan 260 °C, koefisien rendah geseran, dan kos rendah, di antara ciri-ciri lain. Sensitiviti tinggi 104% telah dipaparkan oleh foto-pengesan berdasarkan n-ZnO/p-PAni dan 60% untuk komposit ZnO-10% PAni ke atas substrat PET.

PERFORMANCE OF ZINC OXIDE-POLYANILINE HETEROJUNCTION FOR UV PHOTODETECTION

ABSTRACT

The aim of present study is to fabricate and characterize composites and heterojunction of zinc oxide-polyaniline for UV photodetection application. Initially, photodetectors based on ZnO-PAni composites were fabricated at different concentration of PAni ranging from 5 wt % to 20 wt % using two different methods the first method, photodetector based on twin (ZnO-PAni) composites deposited on porous silicon (PS) substrates. In the second method, UV photodetector based on microparticles of ZnO-PAni composites deposited on glass, polyethylene terephthalate (PET), and silicon (Si) substrates was fabricated. Chemical bath deposition (CBD) method was used to synthesize ZnO (NRs) on glass, PET, and Si substrates. All these device structures were characterized for UV photodetection using platinum (Pt) electrodes. The results showed that addition of PAni in the composite did not alter the hexagonal structure of ZnO phase, but the size of crystal rod of ZnO increased in width with increasing concentration of PAni. The sensitivity of the UV photodetector of microparticles ZnO with 10 wt% PAni on Si substrate was 1.5 times greater than that of a ZnO (NRs) array synthesized on Si substrate, 11.5 times greater than that of a twin ZnO with 15wt% PAni composites on PS substrate, and 29.5 times greater than that a p-n junction fabricated by synthesizing n-ZnO (NRs) on p-polyaniline (PAni) on a SiO₂/Si substrate. Performance of all the fabricated photodetectors was correlated with the structural, surface morphology, substrates, and the optical characteristics of the materials used and the process of photodetection was discussed. The photosensitivity of ZnO-PAni composites could be enhanced much more than ZnO device when they

were irradiated with UV light, one reason is that ZnO-PANI composites showed a stronger absorption in the UV region because both ZnO and PANi can be absorbed by the UV light and another important reason is that PANi in the ZnO-PANI composites can contribute to the generation of more free electrons excitation in the ZnO owing to the existence of p-n junctions in the ZnO-PANI composites. The high photosensitivity of ZnO-PANI composites on Si substrates could be due to photon absorption in the ZnO-PANI composite layer, whereby some of photo generated electrons may diffuse to the ZnO-PANI/Si junction and subsequently were swept into the Si side. In general, both layers may contribute to the photocurrent, which leads to a higher sensitivity of the ZnO-PANI/Si photodetector when compared to the ZnO-PANI composite on the insulator substrate (glass and PET). However, the successful fabrication of high quality, vertically aligned ZnO nanorods/polyaniline heterojunctions and microparticles ZnO-PANI composites on PET flexible substrates, by investigating their applicability as flexible light sensors, that plays an increasingly paramount role in optoelectronics applications. This is due to exceptional properties of PET flexible substrate, which include its dielectric, corrosion resistance, high processing temperature between 196 and 260 °C, low coefficient of friction, and low cost among other credentials. The high sensitivity of 104% has been shown by the photodetector based n-ZnO/p-PANI and 60% for ZnO-10% PANi composite on PET substrate.

CHAPTER 1: INTRODUCTION

1.1 Introduction

Composites of polymer and inorganic material with specific properties are gaining more attention for various applications. There are three main preparations procedures which can be employed to obtain polymer-inorganic composites, namely direct mixing of two or more components in solvent, in situ polymerization of monomer units in presence of inorganic particles and dissolve mixing of polymer with inorganic particles [1, 2]. Incorporation of inorganic component such as ZnO into polymer matrices could result in the modification of the optical, electrical and mechanical properties of the respective components [3, 4]. The first polymer-inorganic composites was reported in early 1960s by Blumstein [5] which was prepared by polymerization of methyl methacrylate in the presence of clay.

Polyaniline (PAni) is one of the most studied organic based conducting polymer which shows ideal properties to be used because of its low cost, simple preparation procedure, good environmental stability, and easily doped behavior. It is a p-type conducting polymer which can be produced as powder [6], thin films [7], or fibers [8].

Zinc oxide (ZnO) as n-type semiconductor is one of the versatile inorganic compound that can be used in many applications because of its low cost and can be readily produced in various forms such as nanowires [9], nanoflowers [10, 11], nanosheet [12], and nanorods [13, 14].

The p-n heterojunction is the key technology for the application of optoelectronic and electronic devices. Thus, heterojunction devices based on n- type

inorganic materials (TiO₂, ZnO, CdSe, and CdS) and p-type organic semiconductor (conducting polymers such as PAni) have acquired much attention for numerous electronic applications [15].

Ultraviolet (UV) photodetectors based on semiconductor have found ways in many applications such as water sterilization, human traffic safety, flame sensing, and pollution monitoring systems [16, 17]. These photodetectors can be constructed into different device structures such as photoconductors and photodiodes:

Photoconductors: It consists of semiconductor with two Ohmic contacts. When a device is exposed to light (with photon energy larger than the energy band gap of the semiconductor) an electron-hole pair would be produced, and the electrical conductivity of the semiconductor is modified. The schematic of the photoconductor is shown in Fig 1.1.

Metal-Semiconductor-Metal (MSM) photodiodes: This consists of two back-to-back Schottky diodes with an inter-digitated electrode arrangement on top of an active light collection semiconductor region. A schematic diagram of the MSM photodiodes is shown in Fig 1.2.

p-n junction photodiode: It comprises a p-n junction that permit light penetration into the region at the vicinity of the metallurgical junction. The schematic of p-n photodiode is illustrated in Fig 1.3.

MSM photodiodes are commonly used as UV photodetectors due to low capacitance per unit area, high response speed, low dark current, and possible zero-bias operation. Also, p-n photodiodes have the advantages of fast responding speed, low dark current, and can be used without applied bias.

The UV region can be divided into four spectral regions [18]: (UV-A: 400-320 nm), (UV-B: 320-280 nm), (UV-C: 280-200 nm) and (Vacuum UV: 200-10 nm). For wider applications, there is a need to develop photodetectors that can be used in wider UV spectral range for wide ranging applications such as environmental, chemical and biological analysis, optical commutation astronomy[18].

Most UV lights are absorbed by the ozone layer. UV wavelengths longer than 280 nm can penetrate the atmosphere and reach the Earth. Thus, UV photodetectors with high sensitivity, fast response and fall times and reproducible characteristics to UV-A, UV-B, UV-C and far UV radiation are required.

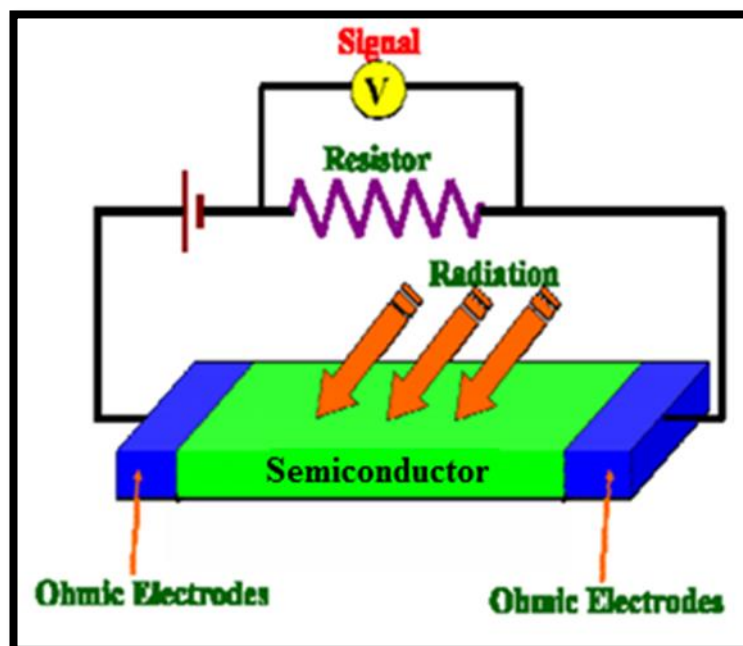


Figure 1.1: The schematic structure of photoconductor [19].

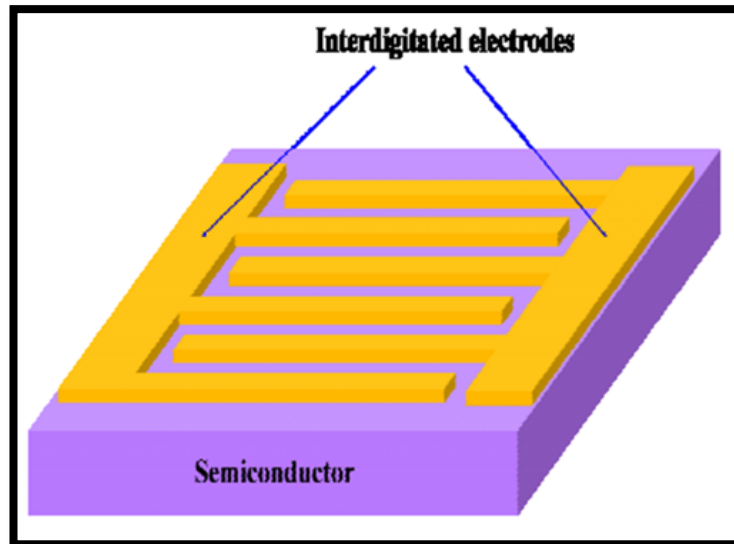


Figure 1.2: The schematic of MSM photodiode structure [19].

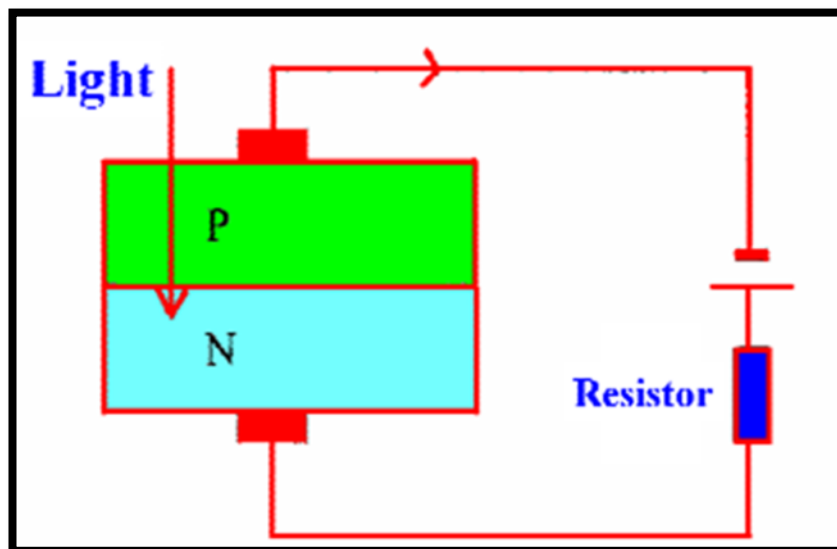


Figure 1.3: The schematic of p-n junction photodiode [19].

1.2 Motivations and Problem statement

Composites and p-n Junction from conducting polymer and metal oxide have been synthesized for applications as gas sensors [20], humidity sensors [21-23], biosensors [24], and photo sensors [25]. However, conducting polymer/ metal oxide composites-based sensors are relatively new and more studies are needed to evaluate the effects of preparation condition and physical properties towards the performance

of photodetector. The most popular composite system is the hybrid inorganic/organic composite, which is formed by inserting inorganic particles to the polymer chain structure to obtain new properties [2, 26, 27]. Although many reports on ZnO-PAni composites can be found in the literature [28-33], the fabrication of ZnO with different wt% of PAni composites on different substrates with particular characteristics and UV detection application, has not been reported so far. So, further investigation should be conducted on the preparation of twin-structure ZnO-PAni composite to elucidate its characteristics for UV applications due to increase the surface area to volume ratio and the PAni acts as a quencher of defects in ZnO where the hydrogen from PAni combines with the oxygen vacancy on the surface of the rod. Interestingly, ZnO-PAni composites exhibit the ability to suppress a broad visible emission band and enhance ultraviolet emission. Thus, it will enhance the ability of zinc oxide as an absorbers of UV light in order to develop their performance and their sensitivity to UV illumination.

Photodetector based on n-ZnO and p-type PAni heterostructures or layer-by-layer have been reported in the literature [34-37]. However, most of the reported ZnO NRs/polymer based heterostructures are made through surface coating of the polymer layer on the NRs. The direct growth of ZnO NRs on conductive polymer substrates is still a challenge with limited success. To this end, chemical bath deposition is a considerably promising approach for growing ZnO nanorods on temperature-sensitive substrates (such as polymers) due to the use of low deposition temperature. Although a large number of studies on organic/inorganic hybrid materials have been reported, they are only focusing on the material preparation and characterization [38, 39] rather than the device assembly and testing. For example, photodetectors can be highly selective to a narrow light wavelength. In recent years, photodetectors have made exceptional progress driven by their exigent need in many applications, such as engine

monitoring, flame detection, chemical sensing, missile plume detection, and inter-satellite communications [40-42]. To date, very rarely work in this area has been reported because of the difficulties in growing nanoscale ZnO on conducting polymer. Herein, to obtain new materials with synergetic or complementary behaviours, light sensing device consisting of vertically aligned ZnO NRs / p-type conducting PANi heterojunction was fabricated to allow the UV light to be implemented through a ZnO(NRs) to the junction and the PANi was selected as the hole conducting layer because of its cheap production in large quantities, stability environmental and easy conductivity control.

The fabrication of ZnO-PAni composites, ZnO(NRs), and n-ZnO/P-PAni junction on polyethylene terephthalate (PET) has attracted huge interest because of its flexibility, light weight, transparency, thinness, transportability, and high resistivity to impact damage which have been used to produce portable devices. With the increasing demand for convenient and portable applications, flexible polymer substrates are more useful when compared with conventional rigid substrates such as silicon, glass and sapphire. Therefore, the use of flexible polymer substrates is being extensively studied for flexible and elastic optoelectronic devices such as smart cards, light emitting diodes, solar cells, and displays.

1.3 Objective of this research

The main objectives of this study can be summarized in the following points:

1- To synthesize twin-structure ZnO-PAni composites by a chemical route with different wt.% of PANi. Also, to synthesize ZnO (NRs) and n-ZnO (NRs) /p-PAni at

different duration time by using low temperature chemical bath deposition (CBD) technique on glass, silicon, and flexible substrates (PET).

2- To study the optimum characteristics of the morphology, structural, and optical properties of the synthesized ZnO-PANI composites, ZnO(NRs), and n-ZnO(NRs)/p-PANI.

3- To fabricate metal-semiconductor-metal (MSM) of the ZnO-PANI composite and n-ZnO/p-PANI heterojunction UV photodetector on glass, PET, and Si substrates.

4- To study the mechanism of twin structure of ZnO and to study the mechanism of the composites between ZnO and PANI.

1.4 Originality of the research

The originality of this research can be summarized through the following points:

1- This work fabricates ZnO-PANI twin-structural composite by chemical method with different weight% PANI, which has not been reported so far.

2- A high-density thin film twin ZnO-PANI composite on PS substrate was produced via spin coating technique for the first time.

3- A UV ZnO-PANI composites based photodetector with high sensitivity and fast photoresponse on different substrate was fabricated.

4- The effects of different growth parameters on the structure of ZnO nanorods synthesized on PANI has been explored for the fabrication of UV photodetectors.

1.5 Scope of study

This work involves preparation of composites from inorganic ZnO and organic conducting polymer of PANi. ZnO nanorods were deposited on PANi via CBD technique for the fabrication of a high-performance UV photodetector on different substrates (glass, Si, PS, SiO₂, and PET).

1.6 Thesis outline

This work is presented in six chapters. Chapter 1 discusses general overview of the subject, motivation, problem statement, thesis objectives, and thesis originality. Chapter 2 provides the literature review and theoretical background of the polymer, conducting polymer, and ZnO semiconductor. In Chapter 3 a detailed description on the methodology and the instrumentation used for the characterization of the materials. Chapter 4 focuses on the characteristics of ZnO-PANi composite and discusses the results of synthesis of nanostructures or microstructures (PS) by electrochemical etching techniques and fabrication processing of UV photodetectors. Chapter 5 presents results related to the growth and characterization of ZnO nanorods on different substrates, the effects of reaction time and substrate by chemical bath deposition on the characteristics of UV photodetector and the growth and characterization of ZnO nanorods grown on PANi. The effects of different growth parameters on the morphology, structure, and optical characteristics of the nanorods and composites as well as the optimal fabrication parameters for the UV photo detectors are given. Finally, conclusions and suggestion for future studies are presented in Chapter 6.

CHAPTER 2: BACKGROUND AND LITERATURE REVIEW

2.1 Introduction

The types of polymers, conducting polymers, its conductivity mechanism and polyaniline (PAni) will be described in this chapter. In addition, the structural properties and the growth mechanism of nanorods and twin ZnO are reviewed. Also, the composite and p-n junction of ZnO-PAni are reviewed. Finally, a review on UV photodetector based on ZnO-PAni and the basic theories of photodetectors are presented.

2.2 Background of polymers

Polymer originates from the Greek word, "poly," which means "many", and "mer," which means "part." Thus, a polymer consists of regularly repeating units called segments that are connected by covalent bonds. Polymers can be classified into several types as follows:

A polymer resulting from polymerization can be distinguished as homopolymers (polymerization of a single monomer) and copolymers (polymeric compound made up of two different types of polymers in the same chain).

In terms of sources, polymers can be distinguished as natural (naturally occurring polymers deduced from plants and animals, such as gum, natural rubber, cotton, wool and leather) or synthetic (polymers produced from simple industrial chemicals, such as synthetic plastics, synthetic rubber, or synthetic fibers).

With regard to the method of synthesis, polymers are sorted out as addition polymers (monomers joined together to provide a single product without loss of any molecule) and condensation polymers (monomers joined together where certain small molecules are removed such as water).

Based on molecular forces acting amidst the molecules, polymers are distinguished as thermoplastic (polymers that soften or melt upon heating, which can be remolded such as Teflon), elastomers (polymers with elastic character such as rubber), and thermosetting (polymers such as polyester that permanently change upon heating; these polymers cannot melt upon heating if the temperature is high enough).

Polymers are also classified as linear (these polymers may tend to fit together uniformly), branched (Polymers with irregular branches along the polymer chain), and cross linked (with branches that make it difficult for polymer molecules to pack in a regular array).

Based on their chemistry, polymers can be classified as organic (Polymers prepared from organic compounds) or inorganic (polymers prepared from non-organic compounds, such as silicon), and element-organic (includes polymers consisting of units containing certain synthetic mineral elements in addition to the presence of some organic groups).

2.3 Background of conducting polymers

Polymers are usually used as insulating and structural materials in packaging and electrical insulations. Combining the advantages of traditional polymers, such as ease of manufacture, lightweight, and low cost, with the electrical properties of semiconductors and metals has been the focus of researchers in the industrial fields for

the past few decades. In 1977, Heeger, et al [43] obtained high conductivity of polyacetylene by doping with I_2 , Br_2 or AsF_5 . Since then, a variety of other conducting polymers and their derivatives have been discovered [44, 45].

Figure. 2.1 shows the molecular structures of some conducting polymers that have been synthesized while Fig 2.2 shows the various application of conducting polymers [46-57]. Conducting polymers are polymers that can conduct electricity upon material charging/discharging. They are called "conjugated polymers" because of the alternating single and double bonds in their polymer chain.

Conjugation in polymers enables some of the π -electrons to be delocalized and shared throughout the polymer. The delocalized electrons may move around the entire system and become the charge carriers that make the polymer conductive. Conductivity in polymers can be divided into two types: i) composites conductivity, which is done by adding conducting particles (usually metallic) to an insulating polymer chain that can be achieved by synthetic method or blending method and ii) conductivity by "doping" where doping of conjugated polymers is usually carried out either by oxidation (p-doped) (removal of electrons) or reduction (n-doped) (electrons adds) of the polymer π -backbone. These cations and anions behave as charge carriers, jumping from one site to another under the effect of an electrical field, thereby increasing conductivity[58]. Conducting polymers can be prepared by electrochemical or chemical methods. Electrochemical polymerization is conducted by working counter and reference electrodes into a solution containing a monomer and an electrolyte and applying a suitable voltage. A polymer film then starts to form on the working electrode, which is normally a metal plate, such as platinum or stainless steel [59]. In chemical polymerization, monomers interact with the excess of the oxidant,

the residue of the interaction is dissolved in a suitable solvent with constant stirring for a certain period.

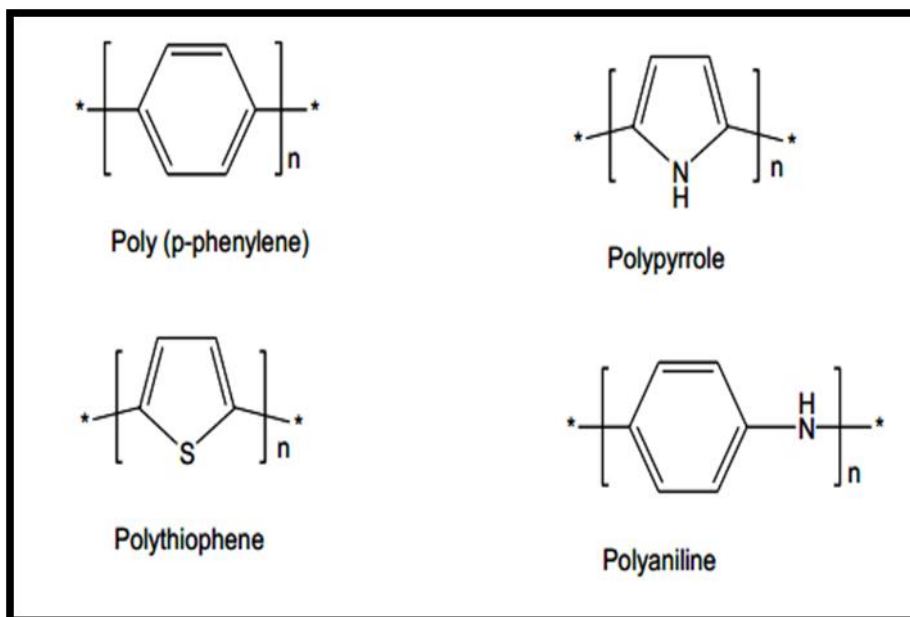


Figure 2.1: Structure of conducting polymers [50].

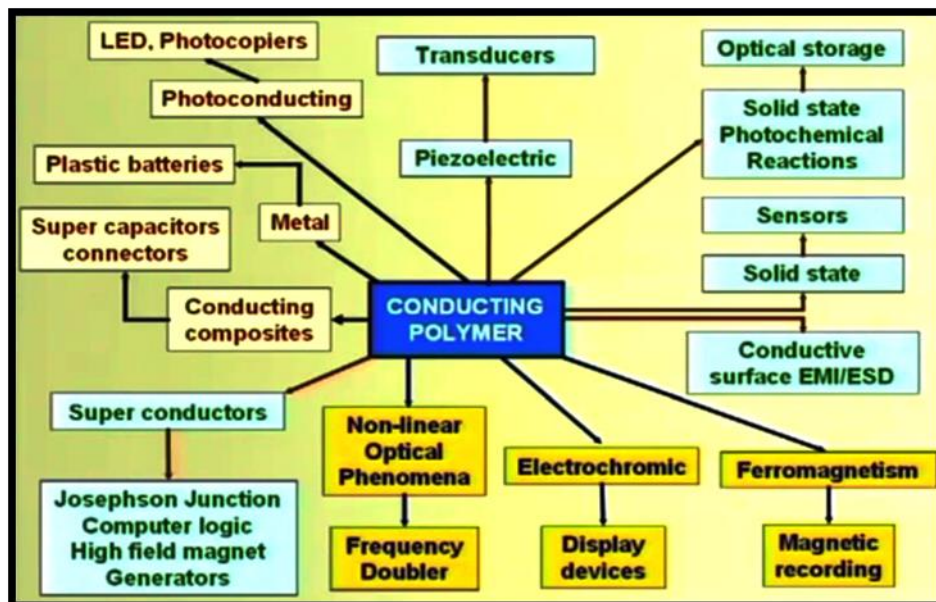


Figure 2.2: Application of conducting polymers.

2.3.1 Conduction mechanism of conducting polymers

The conductivity of conducting polymers starts with insulating and moving towards a more conductive form (metallic), depending on the concentration of the dopant. The conduction mechanism of conducting polymers shows that their behavior is similar to that of a semiconductor, where electrons under thermal excitation jump from the valence band (VB) to the conduction band (CB), thereby providing conductivity[60]. Figure 2.3 shows the band structure of an electronically conducting polymer, where HOMO is the highest occupied molecular orbital and LUMO is the lowest unoccupied molecular orbital. The energy difference between HOMO and LUMO determines the energy gap (E_g). The essential optical properties of these materials is given by the energy gap between the highest occupied π electron band (VB) and the lowest unoccupied band (CB) [61, 62]. This theory is applicable to conductivity if the band gap is narrow. However, this theory is not applicable in the case where the band gap is very wide and the energy required by the electrons at room temperature for their transmission across the gap is not met. Therefore, in addition to the band theory, studying the properties of charge carriers is necessary. The charge carriers, either n-type (electrons) or p-type (holes) can be presented as analogy to the generation mechanism of charge carriers in doped inorganic semiconductors [60]. At low doping levels of polymers, the charge is accommodated in polaron states, whereas at higher doping levels, the charge is accommodated bipolaron (doubly charged defects) transition as shown in Fig 2.4. Both polaron and bipolaron can move along the polymeric chain through rearrangement of the double and single bonds in the conjugated system under an electric field.

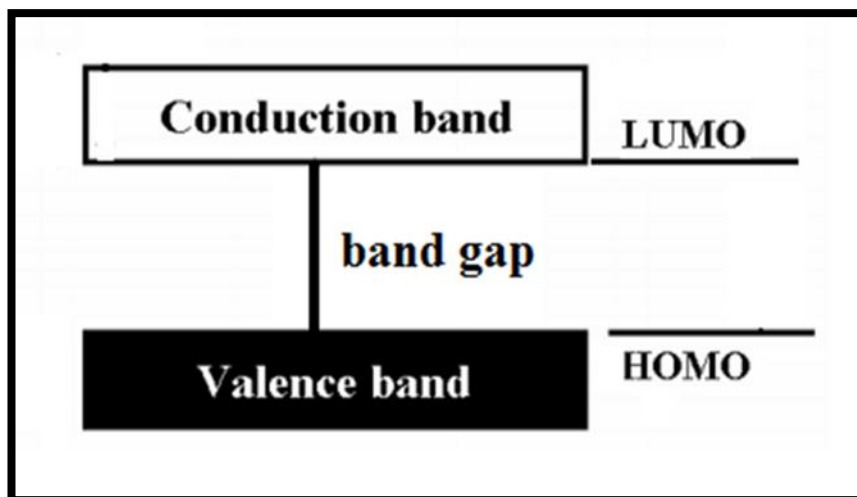


Figure 2.3: Band structure in an electronically conducting polymer.

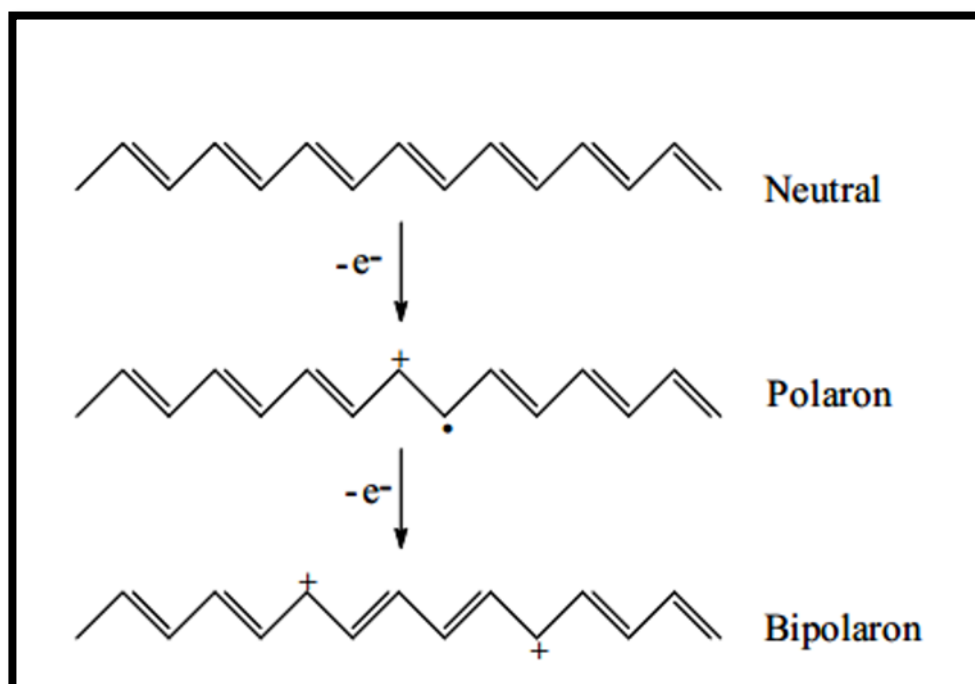


Figure 2.4: Formation of a polaron and a bipolaron for polyacetylene.

2.3.2 Polyaniline (PAni)

Among the conducting polymers, PAni has been intensively studied because of its ease of synthesis, low cost, and environmental stability. PAni which can be produced as bulk powder, cast films, or fibers, shows reversible insulator to metal

electrical behavior depending on its oxidation state and hydrogen ions, i.e. power of hydrogen (PH). PANi is useful for various applications, such as rechargeable batteries [63, 64], light emitting diodes [65, 66], molecular sensors [67, 68], and transistors [69, 70]. Figure 2.5 shows the basic chemical structure of PANi [71]. Each repeat unit contains three benzene rings (symbol 1-3 in Fig 2.5) separated by amine ($-NH$) groups and one quinoid ring (4) connected by imine ($-N=$) groups.

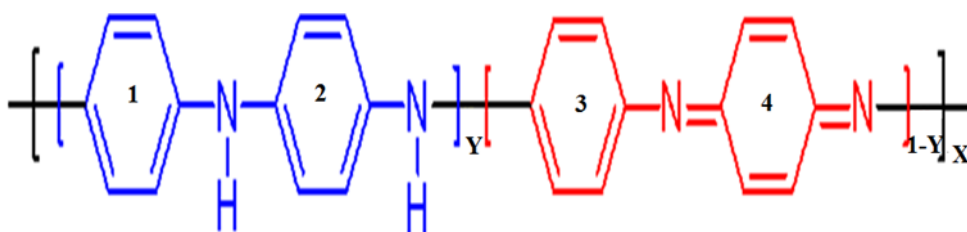
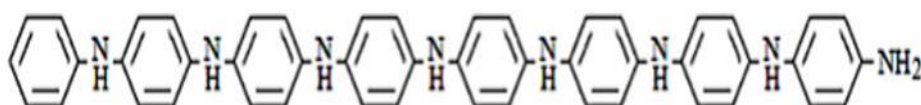


Figure 2.5: The general structure of polyaniline.

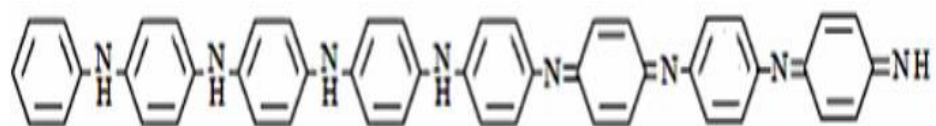
PAni exists in three different forms depending on oxidation states Y [72, 73]:

1) Leucoemeraldine base: fully reduced (all benzenoid units); the value of $Y=1$; has a pale brown color; non-conductive as shown below.



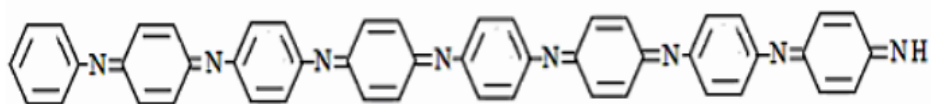
Leucoemeraldine base.

2) Emeraldine base: half oxidized ($Y=0.5$); the number of reduced units is equal to the number of oxidized units, with blue color and does not exhibit conductivity as shown below.



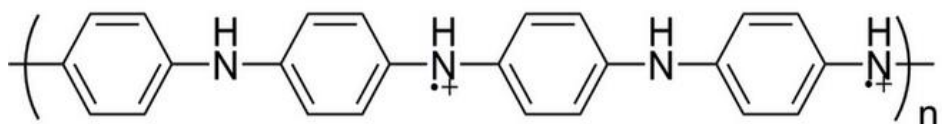
Emeraldine base.

3) Pernigraniline: the value of $Y=0$ (all quinonide); completely oxidized; pink in color; nonconductive as shown below.



Pernigraniline.

The conducting emeraldine salt form can be obtained through acid treatment of the emeraldine form. This state of polyaniline exhibits a dark green color and conductive as shown below.



Emeraldine salt.

PAni is prepared by either electrochemical or chemical oxidation of aniline under acidic condition.

i- Chemical synthesis

Synthesis of PANi chemical oxidative involves the use of either hydrochloride (HCl) or sulfuric acid (H₂SO₄) in the presence of ammonium per sulfate (NH₄)₂S₂O₈ or ferric chloride (FeCl₃), the most commonly used oxidizing agent. In the process of polymerization, the aniline monomer is mixed in aqueous medium with organic acids at 0°C and placed in a magnetic stirrer. Subsequently, the aqueous solution of the oxidant is added to the reaction medium in a drop-wise manner. The precipitate is filtered at the end of polymerization reaction [74-76]. Figure 2.6 shows the chemical polymerization of PANi.

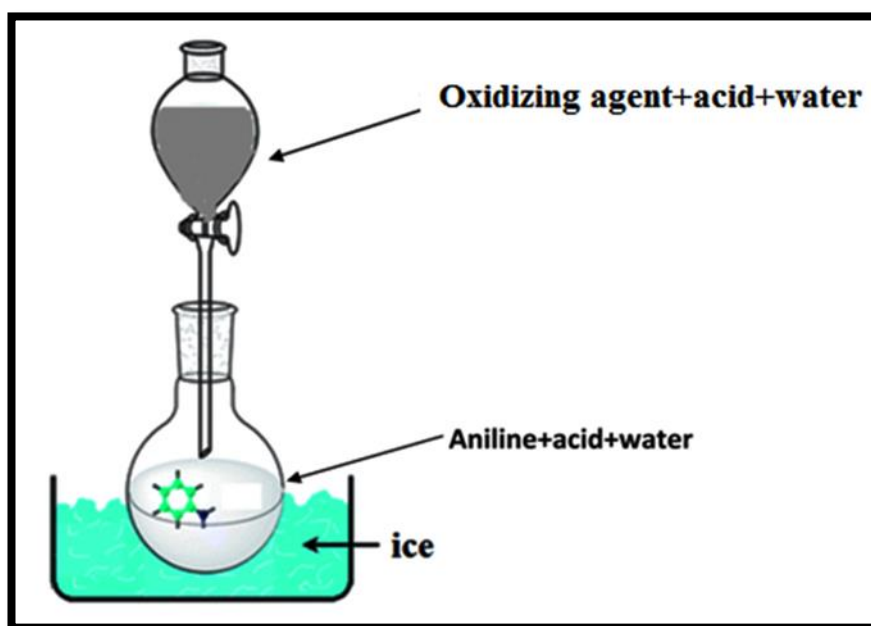


Figure 2.6: Chemical polymerization of PANi.

ii- Electrochemical synthesis

The electrochemical preparation of PANi is generally carried out in an aqueous protonic acid medium. This method can be achieved by employing one of the following techniques [45, 76, 77].

1- Galvanostatic: constant current to an aqueous solution of aniline in the range of 1-10 mA.

2- Potentiostatic: at constant voltage of -0.7 - 1V versus saturated calomel electrode (SCE).

3- Potentiodynamic: variable current and potentials.

A three- electrode assembly is required to carry out electro polymerization using any of the three mentioned techniques. These electrodes are known as counter, reference, and working electrodes (Fig 2.7).

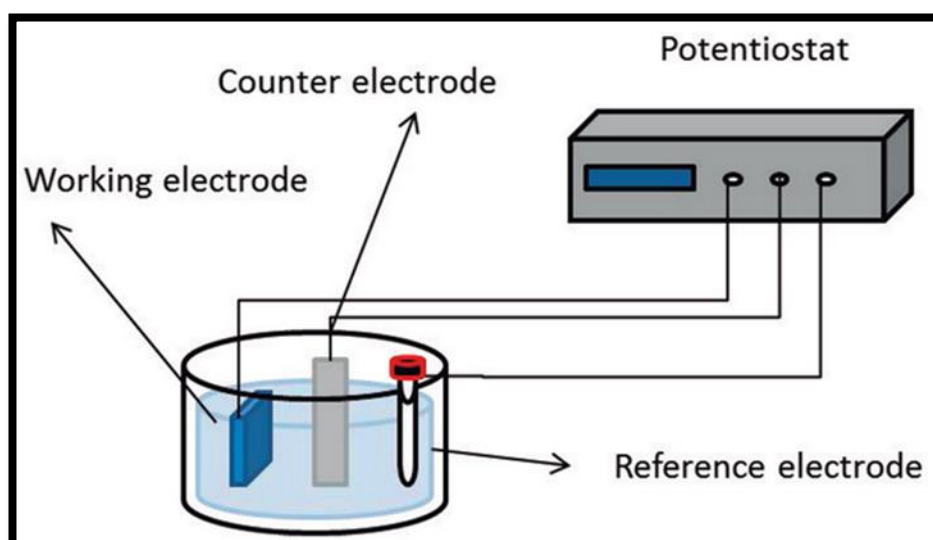


Figure 2.7: Electrochemical polymerization [78].

2.4 Zinc Oxide (ZnO)

Zinc Oxide (ZnO) is an inorganic (metal oxide) semiconductor with either cubic zinc blende (Fig2.8(a)) or hexagonal wurtzite (Fig2.8(b)) structure. Commonly observed hexagonal wurtzite structures have a lattice parameter value at room temperature of $a=b=3.2475\text{\AA}$ to 3.2501\AA and $c=5.2042\text{\AA}$ to 5.2075\AA [79].

ZnO has a large direct band gap of 3.4 eV [80]. With increasing consciousness on environment safety, development of materials that are appropriate for human life and other living forms has gained considerable attention. ZnO is environment friendly and safe to the human body, and thus has been included as an additive in various products in the market, such as white dye paint, food, cosmetics, cement and rubber for car tires. ZnO has become an extensively studied semiconducting material because of its possible applications in light emitting diode (LED) [81], UV detector [82], gas sensor [83], solar cell [84], p-n junction diode [85], and Schottky diode [86]. Undoped ZnO has an intrinsic n-type conductivity, which can easily be increased by doping with Al, Ga, or In [87-89]. The growth of p-type ZnO has been a challenge that has limited the possibility of a p-n homojunction ZnO device.

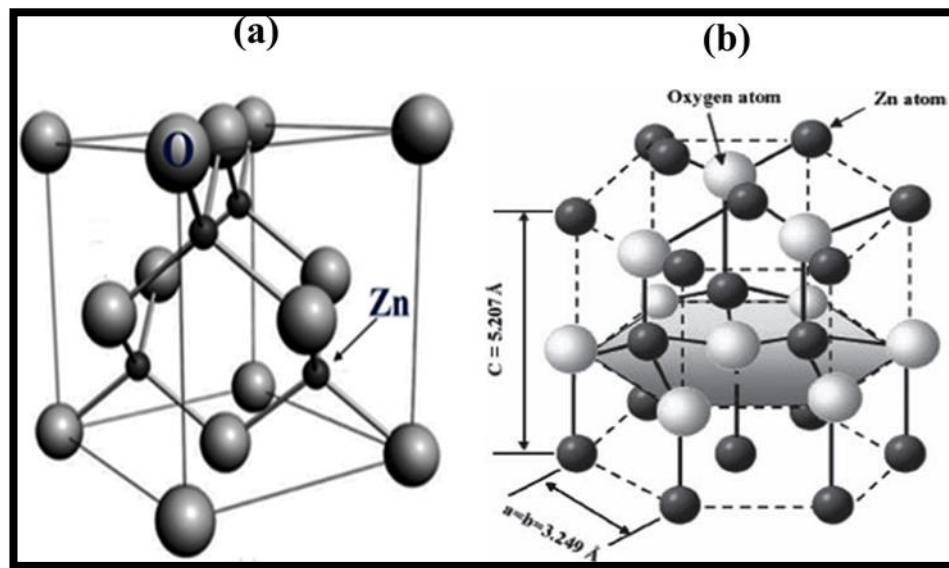


Figure 2.8: Crystal structure of ZnO (a) zinc blend, and (b) hexagonal wurtzite structure [90, 91].

The majority of the optical transition of ZnO nanostructures have been scanned using photoluminescence (PL) spectra at room temperature. The PL spectra of ZnO show two main peaks; a UV emission (around 380 nm) and the emission on the visible

broad peak (around 550 nm) because of impurities. Zinc vacancies (V_{zn}), oxygen vacancies (V_o), zinc interstitials (Zn_i), and so on [92-94], as shown in Fig 2.9. The ratio of the UV peak intensity to the defect peak intensity can be used to characterize the crystalline quality of the ZnO structure.

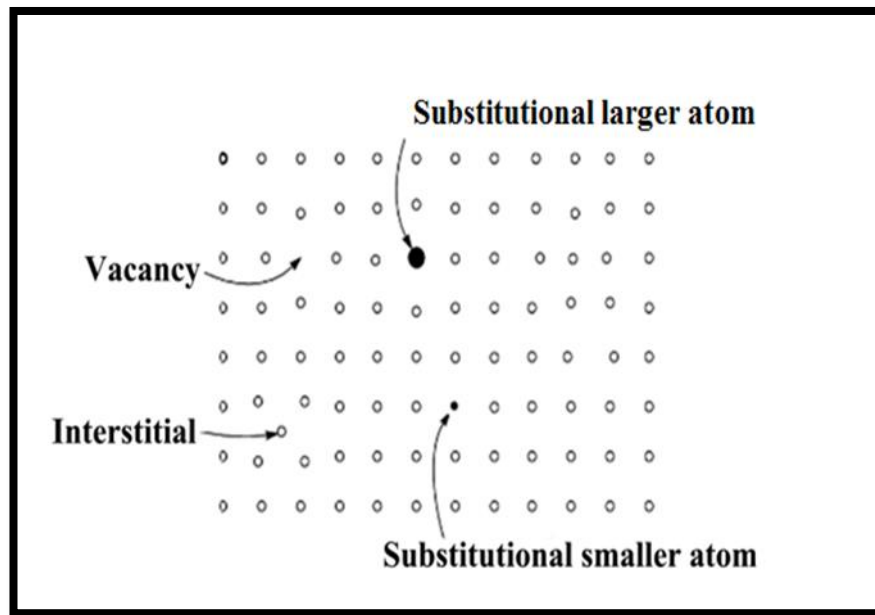


Figure 2.9: Different type of defects in crystalline material.

Several techniques, including vapor-based and solution-based technique, have been introduced to grow ZnO thin film, powders, twin and nanostructure, such as nanorods (NRs), nanoflowers, nanowires (NWs) and nanoparticle (NPs). Low temperature ($<100^{\circ}\text{C}$) and high temperature ($\sim 1000^{\circ}\text{C}$) growth techniques can be differentiated on various kinds of substrates, such as flexible plastic, paper, silicon and sapphire. The most common substrate material used for ZnO growth is sapphire (or Al_2O_3). Silicon is also generally used in the scientific research because this material is much cheaper compared with sapphire. Moreover, a large- sized Si wafer can be obtained and can be cut to any size to fit the deposition requirements of the process. High temperature growth processes, such as chemical vapor deposition (CVD), pulsed